

## Addition of a Block Copolymer to Polymer Blends Produced by Cryogenic Mechanical Alloying

Archie P. Smith,<sup>†,‡</sup> Harald Ade,<sup>\*,‡</sup> Carl C. Koch,<sup>†</sup> Steven D. Smith,<sup>‡</sup> and Richard J. Spontak<sup>\*,†,§</sup>

*Departments of Materials Science & Engineering, Physics, and Chemical Engineering, North Carolina State University, Raleigh, North Carolina 27695, and Corporate Research Division, The Procter and Gamble Company, Cincinnati, Ohio 45239*

*Received September 10, 1999; Revised Manuscript Received November 29, 1999*

**ABSTRACT:** Cryogenic mechanical alloying is used to incorporate a poly(methyl methacrylate-*b*-isoprene) (MI) diblock copolymer into blends of poly(methyl methacrylate) (PMMA) and polyisoprene (PI). Mechanical milling of the copolymer promotes a reduction in the molar mass of the M block, as discerned from glass transition temperature measurements performed by thermal calorimetry, and induces chemical cross-linking of the I block, as determined from sol–gel analysis. These effects become more pronounced with increasing milling time. Morphological characterization of PMMA-rich PI/MI/PMMA blends by X-ray and electron microscopies reveals that the characteristic size scale of the minority phase decreases with increasing MI content, as well as milling time. The nanostructural features observed in such blends are retained at relatively high MI concentrations during subsequent melt-pressing. Impact testing demonstrates that the blends become tougher upon addition of the MI copolymer, even at relatively low copolymer concentrations. Blend toughness likewise increases with increasing milling time up to a point, beyond which phase inversion occurs within the ternary blends (the PI becomes continuous) and impact strength sharply decreases.

### Introduction

Blending two or more homopolymers to obtain a multifunctional multiphase polymer with designer physical and/or chemical properties is one of the most widely used and successful polymer process strategies.<sup>1,2</sup> The inherent immiscibility of most polymers, however, generally precludes the acquisition and retention of fine dispersions desired for optimal, as well as stable, properties. As a result of this complication, numerous methodologies have been developed to reduce the size scale of dispersions in multiphase polymer systems.<sup>3–5</sup> One solution relies on blend compatibilization, which is typically achieved through the addition or in-situ formation of a block (or graft) copolymer. In this regard, block copolymers behave as macromolecular surfactants and migrate to the interface separating adjacent polymer phases. By reducing interfacial tension, the copolymer molecules serve to lessen the driving force for phase separation and suppress phase coarsening.<sup>1,6–8</sup> In most commercial technologies, polymer blends with or without compatibilizing agents are processed in the melt or solution state so that the blend components can be combined and transported at viscosities within equipment tolerance.

A possible alternative to this approach is solid-state mechanical alloying, wherein the constituent polymers are mixed as solids at cryogenic temperatures. Mechanical alloying generally refers to the high-energy ball milling of two or more dissimilar materials to produce homogeneous alloys at the molecular or atomic level,<sup>9</sup>

and is responsible for the ongoing development of novel metastable and nanostructured inorganic alloys possessing interesting mechanical, optical, magnetic, and electronic properties.<sup>9–11</sup> High-energy milling of polymeric materials subjects the blend components to a complex deformation field in which shear, multiaxial extension, fracture, and cold-welding proceed concurrently. This technique has been successfully used to prepare blends of thermoplastics<sup>12–18</sup> and cause allotropism in semicrystalline polymers.<sup>18–20</sup> The dramatically reduced chain mobility in solid-state multicomponent systems effectively prevents phase separation during blending and promotes the formation of nanoscale morphologies. We have previously demonstrated that nanostructured polymer blends composed of poly(methyl methacrylate) (PMMA) and either poly(ethylene-*alt*-propylene) (PEP) or polyisoprene (PI) can be produced by cryogenic mechanical alloying.<sup>21,22</sup>

Another crucial consideration in the mechanical alloying of polymers is the possibility that the chains will undergo scission and generate free radicals that could combine to induce (i) chemical cross-linking of a single polymer species or (ii) chemical coupling of different species. In the latter case, compatibilizing agents would be formed in situ and serve to stabilize nanostructured blends. As detailed elsewhere,<sup>23</sup> PI undergoes chemical cross-linking, and the molecular weight of PMMA can, depending on the initial chain length, decrease sharply upon cryogenic milling. While both observations imply that these macromolecules undergo substantial chemical change during mechanical alloying, no chemical evidence of reactive compatibilization has been observed to date in these PI/PMMA blends, which show signs of limited phase-coarsening when they are subsequently melt-processed at elevated temperatures.<sup>24</sup> To stabilize the nanostructures initially produced during cryogenic mechanical alloying and to reduce the extent of phase

<sup>†</sup> Department of Materials Science & Engineering, NCSU.

<sup>‡</sup> Department of Physics, NCSU.

<sup>§</sup> Department of Chemical Engineering, NCSU.

<sup>‡</sup> The Procter and Gamble Company.

<sup>\*</sup> Present address: Polymers Division, National Institute of Standards & Technology, Gaithersburg, MD 20899.

<sup>\*</sup> To whom correspondence should be addressed.

separation incurred during post-processing, we have incorporated (by co-milling) a daughter poly(methyl methacrylate-*b*-isoprene) (MI) diblock copolymer into solid-state blends of PMMA and PI. In this work, we investigate the morphological characteristics, as well as the mechanical properties, of the resultant ternary blends by using a combination of X-ray and electron microscopies and impact testing.

## Experimental Section

A commercial PMMA homopolymer ( $\bar{M}_n = 252\,000$  and  $\bar{M}_w/\bar{M}_n = 4.11$ ) was obtained from Aldrich, whereas the PI homopolymer ( $\bar{M}_n = 72\,100$  and  $\bar{M}_w/\bar{M}_n = 1.05$ ) and MI diblock copolymer ( $\bar{M}_n = 84\,500$ ,  $\bar{M}_w/\bar{M}_n = 1.05$  and 55 wt % M) were both custom-synthesized via living anionic polymerization. Molecular-weight measurements were conducted by GPC, and the copolymer composition was discerned from  $^1\text{H}$  NMR. Binary PI/PMMA and ternary PI/MI/PMMA blends with 25 wt % isoprene were mechanically alloyed at a cryogenic temperature at which all three materials exist in the solid state. For each milling, 3 g of material (either the copolymer or a blend of predetermined composition), along with 30 g of steel ball bearings measuring 6.4 and 7.9 mm in diameter, was loaded into a hardened steel vial. The vial, sealed under Ar ( $<10$  ppm of  $\text{O}_2$ ), was subsequently placed in a nylon sleeve designed to allow peripheral flow of liquid nitrogen, and the external temperature of the vial was monitored (and maintained below  $-180^\circ\text{C}$ ) throughout milling. The vial assembly was placed in a reinforced SPEX 8000 mill and shaken for milling times ( $t_m$ ) up to 10 h to produce a fine powder. Thermal characterization of the copolymer milled for different times was performed by differential scanning calorimetry (DSC) with a DuPont Instruments 910 calorimeter operated at  $20^\circ\text{C}/\text{min}$  under Ar. Sol-gel analysis of the milled copolymer was performed by vacuum filtration of 0.4 wt % solutions in toluene through Fisher quantitative filter paper Q2 (particle retention  $<1\ \mu\text{m}$ ).

The morphological characteristics and stability of the cryo-milled blends were examined in specimens prepared under various conditions in a Carver press. In one series, powders were pressed at  $20^\circ\text{C}$  and high pressure (700 MPa) for 15 min to retain "as-milled" blend morphologies. To probe the morphologies under melt conditions, samples were also pressed for 5 min at  $125^\circ\text{C}$  (17 MPa) and  $200^\circ\text{C}$  ( $<1$  MPa) and then quenched to ambient temperature. Additional specimens were consolidated for 30 min at  $150^\circ\text{C}$  to probe the morphological evolution of blends annealed for long times at temperatures above the PMMA glass transition temperature ( $T_g$ ). Consolidated plaques were microtomed at  $-100^\circ\text{C}$  in a Reichert-Jung Ultracut S cryoultramicrotome to produce thin sections for scanning transmission X-ray microscopy (STXM) and transmission electron microscopy (TEM). Chemically specific X-ray images of the PI/PMMA and PI/MI/PMMA blends, as well as near-edge X-ray absorption fine structure (NEXAFS) spectra of the neat (unblended) PMMA and PI homopolymers and MI copolymer, were acquired on the microscope located at the National Synchrotron Light Source (Brookhaven National Laboratory). Detailed descriptions of the microscope<sup>25,26</sup> and its use in this study<sup>22</sup> are presented elsewhere. Electron microscopy of blends in which isoprene units were stained with the vapor of 2%  $\text{OsO}_4(\text{aq})$  for 90 min was performed on a Zeiss EM902 electron spectroscopic microscope operated at 80 kV and energy loss settings of 40–120 eV. With ASTM standard testing protocol D256 used as a guideline, Izod impact tests were performed on blends in a Tinius-Olsen model 92T plastics impact tester modified to accept 10 mm samples. Impact samples were prepared by powder compaction at  $20^\circ\text{C}$  and 88 MPa for 5 min, followed by melt-pressing for 5 min at ca.  $40^\circ\text{C}$  above the  $T_g$  of PMMA homopolymer evaluated<sup>23</sup> at  $t_m$  by differential scanning calorimetry. Approximately 15 measurements were conducted per sample, with up to two outlying measurements discarded.

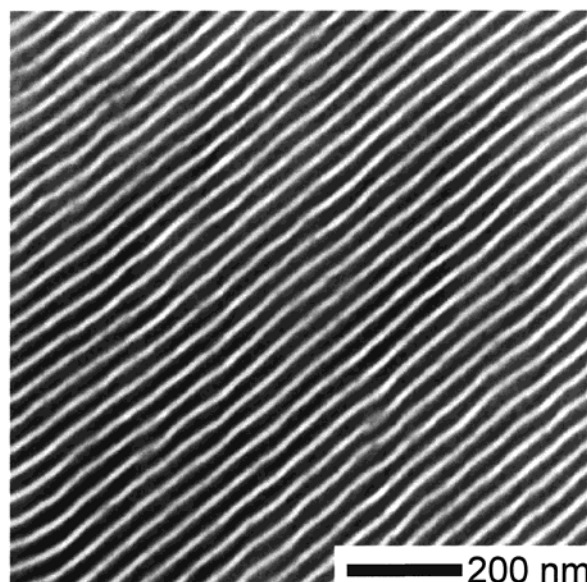


**Figure 1.** TEM image of the poly(methyl methacrylate-*b*-isoprene) (MI) diblock copolymer employed in this study. Isoprene-rich lamellae appear electron-opaque (dark) in this and subsequent TEM micrographs due to selective  $\text{OsO}_4$  staining.

## Results and Discussion

**Block Copolymer Characteristics.** To better understand the role of the MI block copolymer in the PI/MI/PMMA blends, we first turn our attention to the copolymer and its response to high-energy cryogenic milling. Figure 1 is a TEM micrograph of the neat MI copolymer produced by solvent casting from toluene, followed by slow solvent evaporation, annealing, and staining with the vapor of  $\text{OsO}_4(\text{aq})$ . Isoprene-rich regions appear electron-opaque (dark) in this and subsequent TEM images. In light of its composition (55 wt % M) and molecular weight (84 500) and the solubility parameters of PMMA<sup>2</sup> ( $19.5\ \text{MPa}^{1/2}$ ) and PI<sup>27</sup> ( $16.6\ \text{MPa}^{1/2}$ ), this MI copolymer is expected to microphase-order into the lamellar morphology. This morphology, with a period of about 34 nm, is evident in Figure 1 and confirms that the M and I blocks are highly immiscible at the  $T_g$  of the M block, which is measured by DSC (at the midpoint) to be  $138^\circ\text{C}$ . For completeness, the  $T_g$  of the I block in the unmilled copolymer is  $-56^\circ\text{C}$ . It is interesting to note that, while the  $T_g$  for the I block is identical to that of the PI homopolymer ( $-56^\circ\text{C}$ ), the  $T_g$  for the M block in the copolymer is noticeably higher than that for the PMMA homopolymer ( $125^\circ\text{C}$ ).<sup>23</sup> One explanation for this difference lies in the molecular weight polydispersity, which is significantly higher for the PMMA homopolymer. Depending on the molecular weight distribution, short PMMA chains could behave as a plasticizing agent and reduce the  $T_g$  of the homopolymer. This effect is unlikely in the nearly monodisperse copolymer. Another consideration is that commercial PMMA is typically synthesized by free-radical polymerization (and is normally atactic), whereas the M block of the copolymer is the result of living anionic polymerization (and is syndiotactic).

Milling-induced changes in the  $T_g$ 's of the M and I copolymer blocks, as well as of the PMMA and PI homopolymers, are presented as a function of  $t_m$  in Figure 2. Here,  $\Delta T_g$  is defined as  $T_g(t_m) - T_g(0)$ , where  $T_g(0)$  denotes the  $T_g$  of the unmilled material. In the case of the M block, the dependence of  $\Delta T_g$  on  $t_m$  exhibits

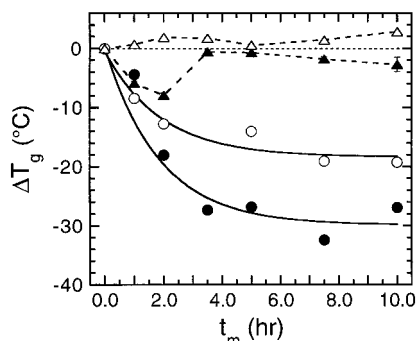


**Figure 2.** Dependence of  $\Delta T_g$  on milling time ( $t_m$ ) for the M (○) and I (Δ) blocks of the MI diblock copolymer, as well as for the PMMA (●) and PI (▲) homopolymers, used in the blends investigated in the present work. The solid lines represent exponential fits to the data,<sup>23</sup> whereas the dashed lines connect the data points.

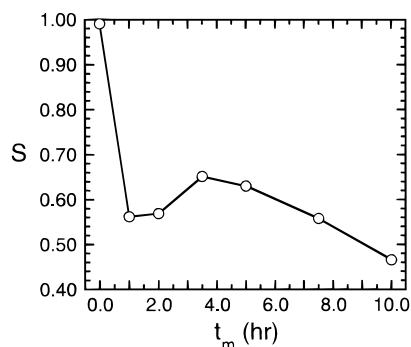


**Figure 3.** Soluble fraction ( $S$ ) of the MI diblock copolymer as a function of  $t_m$ . The solid line connects the data points.

a significant initial decrease in  $\Delta T_g$ , followed by an apparent lower limit, with increasing  $t_m$ . This trend is virtually identical to that observed<sup>23</sup> previously for two PMMA homopolymers differing in molecular weight (one of which is employed in the present study and included for comparison in Figure 2). The minimum value of  $\Delta T_g$  attained for the M block of the copolymer is about  $-19^\circ\text{C}$ , whereas the minimum  $\Delta T_g$  for the PMMA homopolymer subjected to identical cryomilling conditions is measurably lower (ca.  $-28^\circ\text{C}$ ). In marked contrast,  $\Delta T_g$  for the I block of the copolymer is positive at short  $t_m$  and increases further as  $t_m$  increases. Although the magnitude of  $\Delta T_g$  after  $t_m = 10$  h is relatively small (about  $3^\circ\text{C}$ ), it is reproducible and consistent with the dependence of  $\Delta T_g$  on  $t_m$  for the PI homopolymer. As seen in Figure 2,  $\Delta T_g$  for PI decreases at short  $t_m$ , increases abruptly almost to zero, and then decreases with continued milling. Such behavior in the case of the PI homopolymer signifies the onset of chemical cross-linking, as evidenced by sol–gel analysis. The same analysis is conducted here to discern whether comparable milling-induced cross-linking occurs in the MI block copolymer.

The soluble mass fraction ( $S$ ) of the block copolymer is provided as a function of  $t_m$  in Figure 3. At short  $t_m$  (ca. 1 h),  $S$  is found to decrease dramatically. A further increase in  $t_m$  results in values of  $S$  that do not follow any obvious pattern. This behavior differs markedly from that reported<sup>23</sup> earlier for PI, in which  $S$  decreases monotonically with increasing  $t_m$  until the milled homopolymer becomes predominantly insoluble at long  $t_m$ . Such disparity in  $S(t_m)$  between the MI copolymer and PI homopolymer is attributed to differences in the

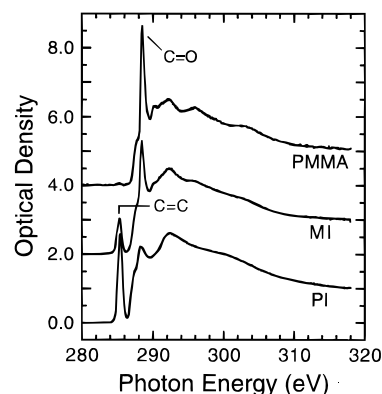


**Figure 4.** NEXAFS spectra of the neat MI copolymer, as well as of the parent PMMA and PI homopolymers. Peaks in the PI and PMMA spectra arise at 285.0 (C=C excitation) and 288.4 eV (C=O excitation), respectively. Because of selective X-ray absorption, PI appears dark relative to PMMA in STXM images acquired at 285.0 eV.

mechanics of milling. The copolymer is inserted into the milling vial as a loose powder and immediately undergoes all the mechanical deformation modes associated with cryomilling. Conversely, the PI homopolymer is deposited into the vial in a large consolidated mass (from solution) that must be broken apart before mechanical forces act upon the entire mass. Relative to the PI homopolymer, more of the MI copolymer is involved in cross-linking at short  $t_m$ , thereby resulting in a sharp initial reduction in  $S$ . While the PI homopolymer eventually becomes nearly insoluble with increasing  $t_m$ , a substantial fraction of the cryomilled MI copolymer always remains soluble since it consists of broken M blocks that cannot cross-link. The observation that the MI copolymer undergoes chemical cross-linking upon cryomilling is important since the I block of the copolymer and PI homopolymer may cross-link and further stabilize nanostructures produced during milling.

**Mechanically Alloyed Blends. NEXAFS Characterization.** To exploit the chemical sensitivity available in STXM, one or more characteristic X-ray absorption energies for each polymer must first be determined from its NEXAFS spectrum. Figure 4 shows the C k-edge spectra acquired from the neat MI copolymer, as well as from the neat PMMA and PI homopolymers. Peaks in these spectra identify energies at which the polymers strongly absorb X-rays. The PI spectrum, for example, possesses a sharp peak near 285.0 eV due to excitations corresponding to C=C bonds in the chain backbone, whereas the PMMA spectrum exhibits a sharp peak at 288.4 eV due to excitation of C=O bonds. As expected a priori, the MI spectrum appears as a combination of the PI and PMMA spectra, with peaks of reduced intensity corresponding to both excitations. A least-squares fit of the PI and PMMA spectra to the composite MI spectrum yields 57 wt % PMMA, which is in favorable agreement with the composition of the copolymer discerned by  $^1\text{H}$  NMR (55 wt % PMMA). On the basis of the spectra provided in Figure 4, PI will appear dark in STXM images acquired at 285.0 eV due to the selectively high absorption of X-rays by PI at this particular photon energy.

**Copolymer Concentration.** X-ray images of blends cryomilled for 5 h and pressed at three different temperatures are presented in Figure 5 for four different concentrations of MI copolymer (in weight percent): 0 (Figure 5a–c), 2 (Figure 5d–f), 6 (Figure 5g–i), and 10



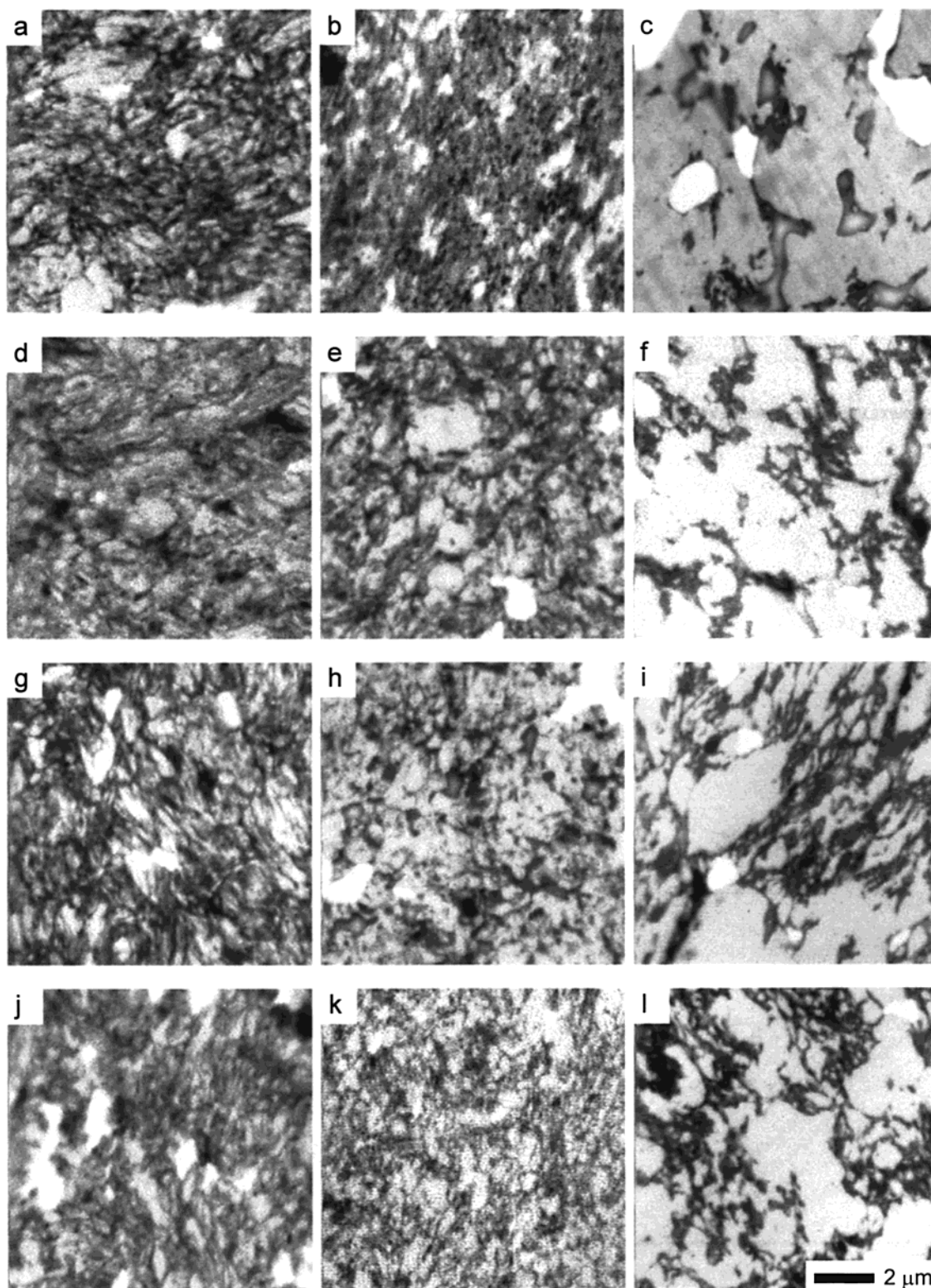


**Figure 5.** STXM images acquired at 285.0 eV (PI dark) from PI/MI/PMMA blends cryomilled for 5 h with different concentrations of copolymer (in wt %): 0 (a–c), 2 (d–f), 6 (g–i), and 10 (j–l). The columns correspond to different pressing temperatures (in °C): 20 (first column; a, d, g, j), 125 (second column; b, e, h, k), and 200 (third column; c, f, i, l). The overall blend composition is 25 wt % isoprene in each case.

(Figure 5j–l). The blends have been consolidated at 20 °C (first column, Figure 5a,d,g,j), 125 °C (second column, Figure 5b,e,h,k), and 200 °C (third column, Figure 5c,f,i,l) for 5 min prior to quenching. In the blends pressed at ambient temperature, mobile PI flows around, and outlines, the glassy PMMA particles so that the blend morphologies appear grossly similar. Such micro-

structural uniformity in these blends is consistent with the intuitive expectations that (i) the PMMA chains are immobile during consolidation at ambient temperature and (ii) the MI copolymer does not function as a compatibilizing agent during cryomilling or post-pressing at 20 °C. Once the blends are heated to 125 °C, which is at the  $T_g$  of the unmilled PMMA, subtle

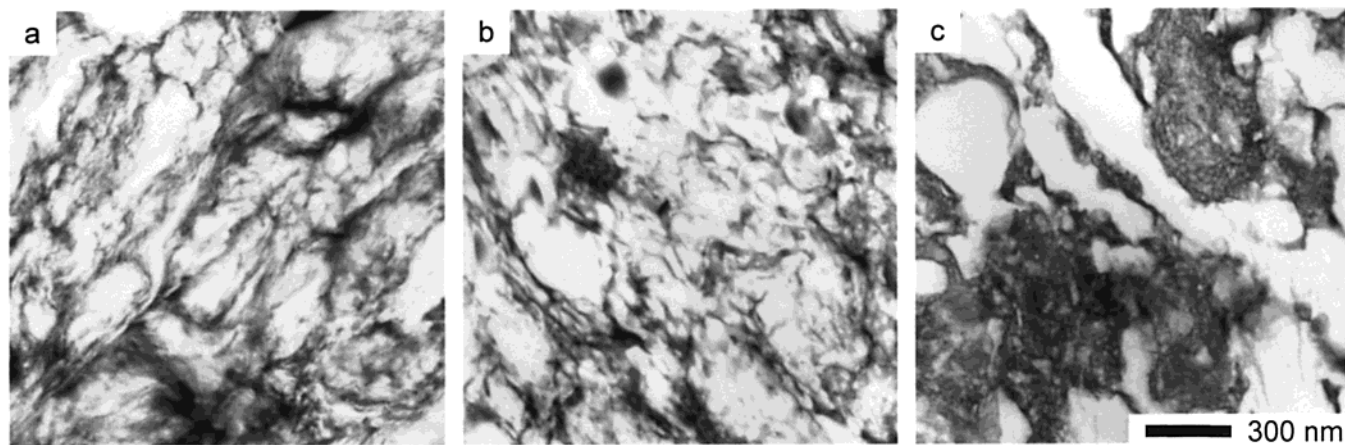


**Figure 6.** TEM images of the 20/10/70 PI/MI/PMMA blends cryomilled for 5 h and melt-pressed at different temperatures (in °C): 20 (a), 125 (b), and 200 (c). As in Figure 1, isoprene-rich regions appear dark due to selective staining.

differences in blend morphology become evident. Addition of block copolymer does not significantly influence blend morphology at this temperature due presumably to the lack of chain mobility in a high-viscosity melt. When the melt-pressing temperature is increased to 200 °C, the morphological features of these blends undergo a pronounced evolution. In the blend with no copolymer (Figure 5c), the PI domains coalesce and attain sizes of up to 4  $\mu\text{m}$  across. As the amount of copolymer is increased, the PI morphology changes from loosely connected domains to a fine semicontinuous morphology in which PI elements measure as small as 200 nm across. At low MI concentrations (Figure 5f), the PI network is not uniformly distributed and exists as pockets within the PMMA matrix. These pockets become more evenly connected, forming a semicontinuous phase within the blend, as the copolymer concentration increases. Comparison of these morphological characteristics suggests that the MI copolymer serves as a compatibilizing agent in PI/MI/PMMA blends heated to temperatures above the PMMA  $T_g$ .

The fine-scale features of these blends are further investigated by TEM. Micrographs of the 20/10/70 PI/MI/PMMA blends cryomilled for 5 h and consolidated for 5 min at 20 (a), 125 (b), and 200 °C (c) are displayed in Figure 6. Close comparison of these micrographs reveals little difference between the morphologies of the blends consolidated at 20 and 125 °C. Both blends exhibit a nearly continuous PI phase possessing nanostructural features as small as 30 nm across. The absence of substantial phase coarsening in the blends pressed at 125 °C is consistent with the data presented in Figure 5 and reflects insufficient molecular mobility for large-scale morphological reorganization at this temperature. Upon pressing the same blend at 200 °C, however, noticeable phase separation is evident (see Figure 6c). While PI still forms a semicontinuous network, many of the fine nanostructural details seen in Figure 6a,b are replaced by large-scale PI-rich domains that contain nanoscale PMMA inclusions measuring as small as 20 nm across.

**Milling Time.** To ascertain the effect of  $t_m$  on blends with the MI copolymer, we have prepared a series of 22/6/72 PI/MI/PMMA blends cryogenically alloyed for up to 10 h. Figure 7 displays STXM images acquired from blends subjected to different  $t_m$  (in hours)—1 (Figure 7a–c), 5 (Figure 7d–f), and 10 (Figure 7g–i)—and consolidated at 20 °C (first column, Figure 7a,d,g),

125 °C (second column, Figure 7b,e,h), and 200 °C (third column, Figure 7c,f,i). As in Figure 5, the morphologies of the blends consolidated at 20 °C represent the “as-milled” powder morphologies, which differ significantly as a function of  $t_m$  in these blends. After 1 h of cryomilling (Figure 7a), relatively large PMMA domains (up to 5  $\mu\text{m}$  across) remain. As  $t_m$  is increased, the size of the PMMA domains decreases substantially to less than 1  $\mu\text{m}$  after 5 h (Figure 7d) and less than 200 nm after 10 h (Figure 7g). Similar results have been reported for PI/PMMA blends without added copolymer,<sup>22</sup> implying that this difference in morphology is due to  $t_m$  and not to the incorporation of copolymer. When the pressing temperature is increased to 125 °C, however, the role of the MI copolymer becomes more apparent. The blend cryomilled for 1 h (Figure 7b) exhibits relatively large, isolated PI domains dispersed within PMMA. In contrast, PI forms a semicontinuous network in the blend milled for 5 h (Figure 7e), and no obvious sign of phase separation is evident in the blend cryomilled for 10 h (Figure 7h). As discussed earlier with regard to Figure 6, the morphologies of the blends milled for 10 h and consolidated at 20 and 125 °C appear strikingly similar.

An increase in the consolidation temperature to 200 °C is accompanied by significant differences in blend morphology. After 1 h of cryomilling (Figure 7c), the PI phase elements coalesce to form larger domains within the PMMA matrix. These PI domains become as large as 4  $\mu\text{m}$  in size and contain PMMA inclusions measuring as large as 0.5  $\mu\text{m}$  across. The PMMA inclusions are attributed to the MI copolymer, since PMMA inclusions are not observed<sup>22</sup> for identical samples without the copolymer. As  $t_m$  is increased, the PI phase again adopts a semicontinuous morphology in PMMA. The morphology of the blend milled for 5 h (Figure 7f) has been discussed earlier with regard to Figure 5, whereas the network morphology formed in the blend milled for 10 h (Figure 7i) appears more uniformly distributed. Electron micrographs of the blends milled for 10 h are presented in Figure 8 for completeness. The blend consolidated at 20 °C (Figure 8a) exhibits little evidence of gross phase separation. Melt-pressing at 125 °C (Figure 8b) promotes local refinement of PI nanoscale domains typically measuring 30 nm across. Increasing the temperature to 200 °C (Figure 8c) induces formation of a semicontinuous PI network in which PMMA domains as small as 20 nm are embedded. Figures 7 and



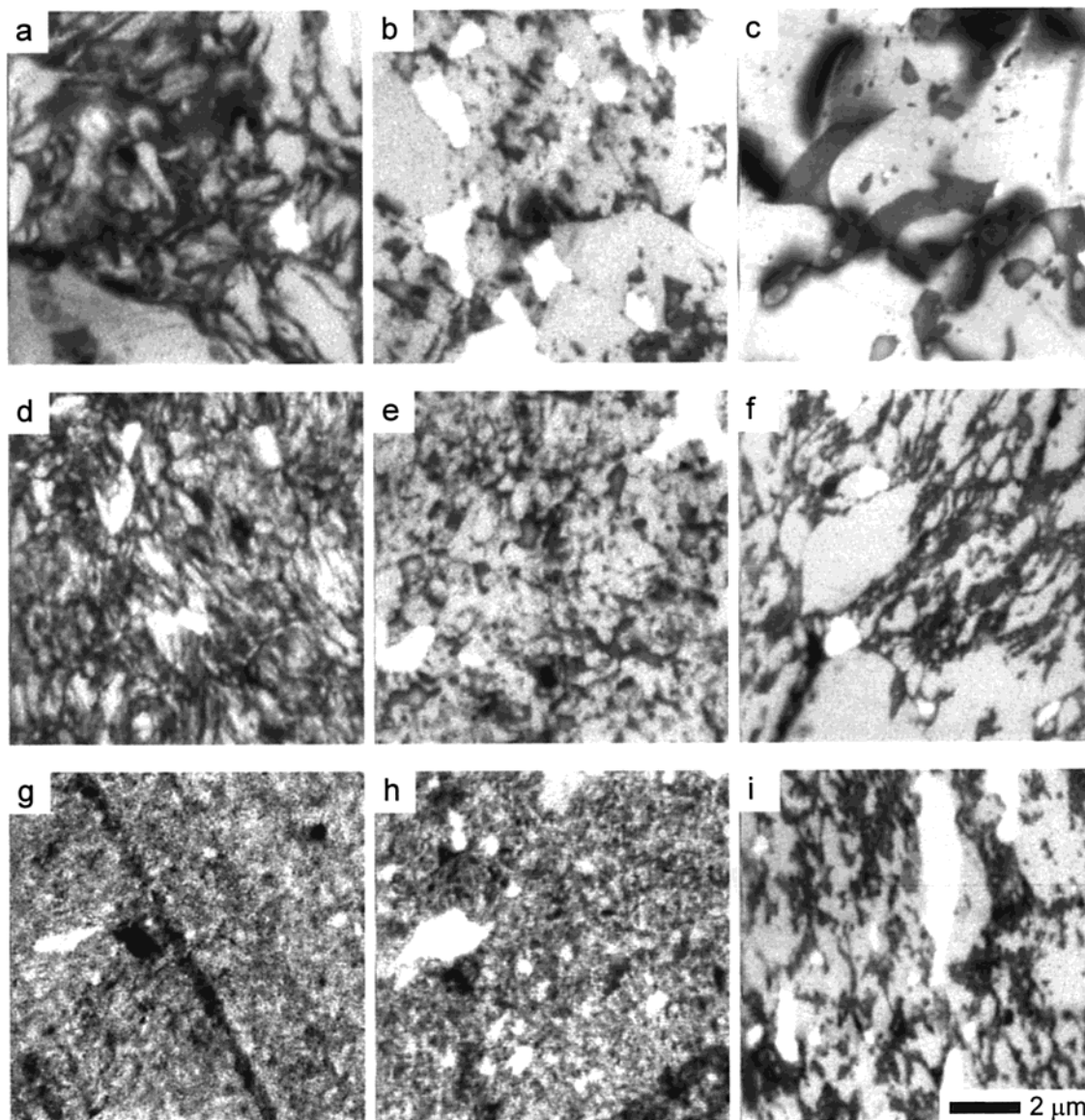


**Figure 7.** STXM images acquired at 285.0 eV (PI dark) from 22/6/72 PI/MI/PMMA blends cryomilled for different  $t_m$  (in h): 1 (a–c), 5 (d–f), and 10 (g–i). The columns correspond to different pressing temperatures (in °C): 20 (first column; a, d, g), 125 (second column; b, e, h), and 200 (third column; c, f, i).

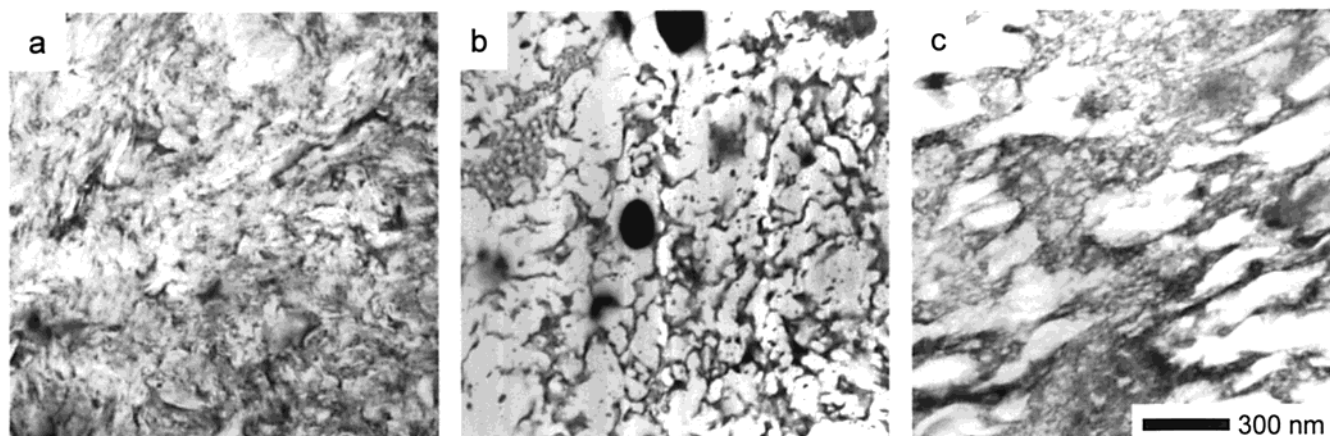


**Figure 8.** TEM images obtained from 22/6/72 PI/MI/PMMA blends cryomilled for 10 h and melt-pressed at different temperatures (in °C): (a) 20, (b) 125, and (c) 200. For the blend consolidated at ambient temperature, PI appears finely dispersed throughout the PMMA matrix. At higher temperatures, the PI forms discrete domains at 125 °C and a semicontinuous network at 200 °C.

8 clearly demonstrate that  $t_m$  has a profound effect on the morphology of these blends by generating finer phase elements as  $t_m$  is increased. Incorporation of the

MI copolymer within these blends also serves to reduce (and stabilize) the I-rich domains in these blends relative to blends without copolymer.

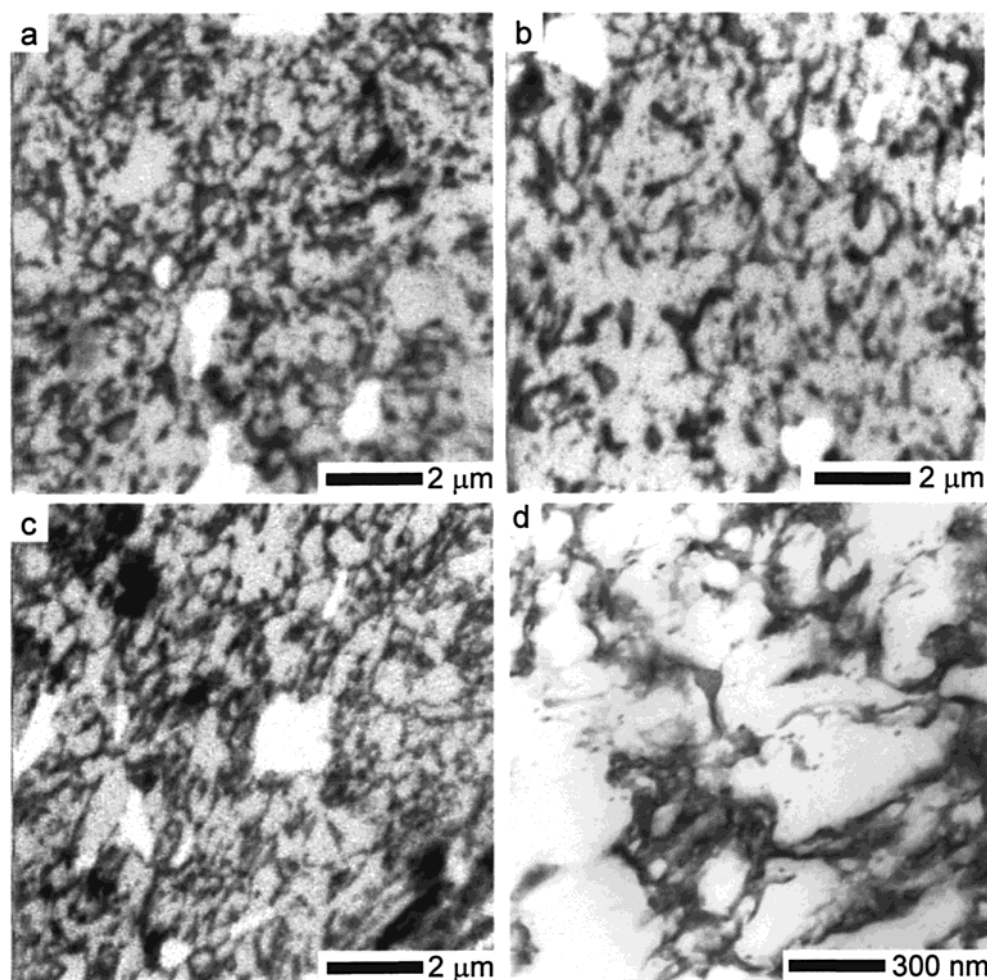


**Figure 9.** STXM (a–c, 285.0 eV) and TEM (d) images acquired from PI/MI/PMMA blends cryomilled for 5 h with different concentrations of copolymer (in wt %): 2 (a), 6 (b), and 10 (c, d). The blends have been annealed for 30 min at 150 °C.

**Thermal Annealing.** Phase-coarsening in PI/MI/PMMA blends is examined here as a function of MI copolymer concentration by annealing blends for 30 min at 150 °C. The morphologies of blends cryomilled for 5 h, as discerned by STXM, are presented in Figure 9 for three different MI concentrations (in weight percent): 2 (Figure 9a), 6 (Figure 9b), and 10 (Figure 9c). In the blend with 2 wt % copolymer, the morphology appears as a fine semicontinuous PI network. Careful comparison of this image and its complementary image obtained at 288.4 eV (PMMA dark, not shown) reveals that this interpretation of the morphology is misleading.<sup>28</sup> Instead of a network-like PI phase in which PMMA is embedded, the PI forms relatively large dispersions ( $\approx 1 \mu\text{m}$  across) that have thinned in the microtomed sections so that they are of comparable chemical contrast as PMMA. The morphology in this blend is actually quite coarse and indicates that little copolymer-induced compatibilization has been achieved, which is consistent with the low quantity of MI present. In the blend with 6 wt % copolymer (Figure 9b), the PI morphology becomes finer and better dispersed, with significantly less thinning. As the MI concentration is increased to 10 wt % (Figure 9c), the PI forms semicontinuous domains containing nanoscale PMMA inclusions. Figure 9d displays a TEM micrograph of the blend presented in Figure 9c so that nanoscale features are more clearly visible. The PMMA inclusions inside the PI domains, as well as some of the PI features, measure as small as 20 nm across.

Also of interest is the morphological evolution of blends alloyed for different  $t_m$ , which is shown for 22/6/72 PI/MI/PMMA blends in Figure 10. In this figure, STXM images are displayed for blends annealed for 30 min at 150 °C and subjected to different  $t_m$  (in hours): 1 (Figure 10a), 5 (Figure 10b), and 10 (Figure 10c). Consistent with the images shown in Figures 7 and 8, this figure illustrates the importance of  $t_m$  on blend morphology. In the case of the blend milled for 1 h (Figure 10a), the PI forms isolated domains ranging in size from 200 nm to 2  $\mu\text{m}$  across within a PMMA matrix, confirming that little, if any, compatibilization is achieved during this short  $t_m$ . The morphology of the blend milled for 5 h (Figure 10b) has been previously discussed with regard to Figure 9. Upon increasing  $t_m$  further to 10 h (Figure 10c), the PI forms a nearly continuous phase in which regions of PMMA are dispersed. The fine features of this morphology, such as 20 nm PI channels, are evident in the TEM image provided in Figure 10d. The images in Figure 10 demonstrate that nanoscale morphologies are not only achieved with cryogenic mechanical alloying but also retained during subsequent melt processing.

**Impact Strength.** Izod impact testing has been performed on blends discussed in the previous section to ascertain the effect of mechanical alloying on physical properties. Impact strength is presented in Figure 11 as a function of MI concentration for blends cryomilled for 5 h and melt-pressed at the conditions specified in the Experimental Section. Addition of the MI copolymer



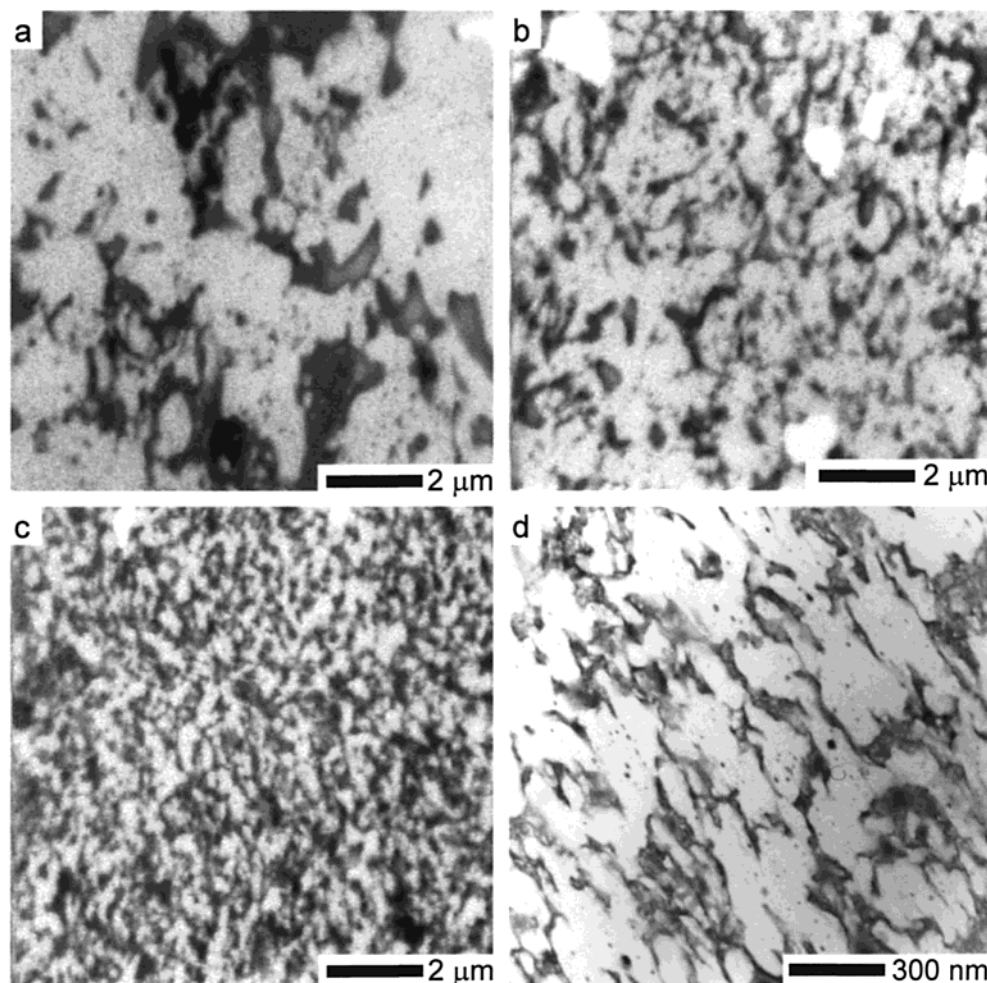


**Figure 10.** STXM (a–c, 285.0 eV) and TEM (d) images collected from 22/6/72 PI/MI/PMMA blends cryomilled for different  $t_m$  (in h): 1 (a), 5 (b), and 10 (c, d). As in Figure 9, the blends have been annealed for 30 min at 150 °C.

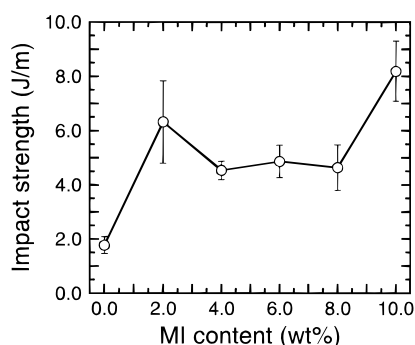


**Figure 11.** Variation of impact strength with MI copolymer concentration for PI/MI/PMMA blends cryomilled for 5 h and melt-pressed for 5 min at the conditions described in the text. The solid line connects the data points, and the error bars denote one standard deviation in the data.

promotes a noticeable improvement in the impact strength of these blends even at relatively low concentrations (2 wt %) of copolymer. This improvement, remaining relatively constant up to 8 wt % copolymer, may reflect the number of molecules that are capable of chemically cross-linking during cryomilling. In the absence of copolymer, PI can only cross-link with itself. Upon addition of copolymer at constant blend composition (25 wt % isoprene and 75 wt % methyl methacrylate), the MI copolymer and PI homopolymer can inter-cross-link and toughen the PMMA matrix. According to

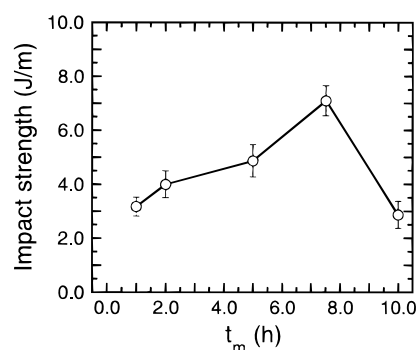


**Figure 12.** Dependence of impact strength on  $t_m$  for 22/6/72 PI/MI/PMMA blends. The solid line connects the data points, and the error bars denote one standard deviation in the data.

Figure 11, a second increase in impact strength arises when the concentration of MI copolymer reaches 10 wt %. While this increase is not yet fully understood, the images displayed in Figure 5j–l reveal that, unlike the other blends examined here, blends with 10 wt % copolymer appear quasi-homogeneous under some milling/pressing conditions. It is certainly conceivable that single-phase behavior may favorably affect the impact strength of the blend. Figure 12 shows the dependence of blend impact strength on  $t_m$  for blends with 6 wt % copolymer and demonstrates that as  $t_m$  is increased, impact strength increases steadily up to 8 h but drops



off sharply at 10 h. This result is attributed to the decreasing size of the PI phase with increasing  $t_m$ , as seen in Figures 7 and 8. As  $t_m$  is increased, PI domains remain essentially isolated and strengthen the matrix (most of them lie in the size range established<sup>29–32</sup> for rubber-toughened PMMA). Once  $t_m$  reaches 10 h, however, the PI domains form a fine, nearly continuous network, in which case impact testing measures the toughness of the PI, rather than PMMA, phase.

## Conclusions

The purpose of this study is to discern the effect of adding a nearly symmetric MI block copolymer to blends of PMMA and PI produced by cryogenic mechanical alloying. The neat MI copolymer is microphase-ordered, exhibiting the lamellar morphology, at the  $T_g$  of the M block. High-energy mechanical milling of this copolymer yields a reduction in the measured  $T_g$  of the M block, indicating that the mass of the M block decreases during milling. In contrast, the variation in the  $T_g$  of the I block, as well as in the soluble fraction of copolymer, with milling time reveals that the I block undergoes milling-induced chemical cross-linking. This observation implies that the MI copolymer and PI homopolymer will most likely inter-cross-link during the cryogenic alloying of PI/MI/PMMA blends. Such processing-induced molecular modification is atypical of conventional polymer blends. Morphological characterization of these ternary blends indicates that the copolymer promotes some degree of emulsification once the post-processing temperature is sufficiently high to reduce the matrix viscosity and enable chain migration. At consolidation temperatures near 200 °C, the morphologies of blends without the MI copolymer consist primarily of PI domains measuring up to 5  $\mu\text{m}$  across, whereas identical blends with 10 wt % copolymer possess a semicontinuous PI network with features measuring as small as 20 nm.

In addition to composition and consolidation temperature, another important consideration affecting blend morphology is milling time. As the milling time is increased, the mechanical action of alloying uniformly distributes the block copolymer to produce blends with finer morphologies than observed for blends without copolymer. In blends cryomilled for 10 h, the morphology produced is almost spatially invariant, with both PI and PMMA phases measuring on the order of 100 nm in size. The presence of the copolymer is responsible for not only a reduction in the size of I-rich phase elements within the blends but also retention of such morphologies upon annealing at elevated temperatures (above the PMMA  $T_g$ ). Blends with 2 wt % MI copolymer possess PI domains as large as 1  $\mu\text{m}$  across, whereas the PI in blends with 10 wt % copolymer forms a semicontinuous network, again with features measuring ca. 20 nm across. Impact testing of these blends confirms that the addition of copolymer to these blends results in a significant improvement in impact strength, even at low copolymer concentrations. In addition, the impact strength is found to increase steadily with increasing milling time until a continuous PI phase is formed, at which point the impact strength drops precipitously.

Results presented here indicate that the addition of a block copolymer to blends produced by cryogenic mechanical alloying promotes limited compatibilization during post-processing. Although mechanical alloying does not appear to distribute the copolymer along the

polymer–polymer interface where it would be of most use in the present ternary system, sufficient dispersion appears to be achieved during alloying so that when chains can migrate, emulsification occurs, resulting in a reduction in phase-coarsening and an improvement in physical properties. Comparable, if not more promising, results are anticipated in other polymer blends in which the constituents are less sensitive to milling-induced molecular degradation than PMMA. Cryogenic mechanical alloying followed by melt compatibilization constitutes an interesting alternative to producing novel polymer blends (especially when conventional melt and solution processes are not suitable) and warrants further investigation.

**Acknowledgment.** X-ray microscopy data were collected using the Stony Brook STXM instrument developed by the group of J. Kirz and C. Jacobsen at SUNY Stony Brook, with financial support from the Office of Biological and Environmental Research, U.S. DOE, under Contract DE-FG02-89ER60858, and the NSF, under Grant DBI-960-5045. S. Spector and C. Jacobsen of SUNY Stony Brook and D. Tennant of Lucent Technologies developed the zone plates with support from the NSF under Grant ECS-951-0499. A NSF Young Investigator Award (DMR-945-8060) supports H.A. and A.P.S. We thank A. G. Erlat and D. A. Winesett for technical assistance.

## References and Notes

- (1) Utracki, L. A. *Polymer Alloys and Blends*; Carl Hanser Verlag: Munich, 1990.
- (2) Sperling, L. H. *Polymeric Multicomponent Materials*; John Wiley & Sons: New York, 1997.
- (3) Macosko, C. W.; Guegan, P.; Khandpur, A. K.; Nakayama, A.; Marechal, P.; Inoue, T. *Macromolecules* **1996**, *29*, 5590.
- (4) Bouilloux, A.; Ernst, B.; Lobbrecht, A.; Muller, R. *Polymer* **1997**, *38*, 4775.
- (5) Feng, Y.; Weiss, R. A.; Han, C. C. *Macromolecules* **1996**, *29*, 3925.
- (6) Bates, F. S. *Science* **1991**, *251*, 898.
- (7) Lyatskaya, Y.; Gersappe, D.; Balazs, A. C. *Macromolecules* **1995**, *28*, 6278.
- (8) Piirma, I. *Polymer Surfactants*; Dekker: New York, 1992.
- (9) Koch, C. C. In *Materials Science and Technology*; Cahn, R. W., Ed.; VCH: Weinheim, 1991; Vol. 15, p 583.
- (10) Lu, L.; Lai, M. O. *Mechanical Alloying*; Kluwer Academic: Norwell, MA, 1998.
- (11) Murty, B. S.; Ranganathan, S. *Int. Mater. Rev.* **1998**, *43*, 101.
- (12) Pan, J.; Shaw, W. J. D. *Microstruct. Sci.* **1993**, *20*, 351.
- (13) Pan, J.; Shaw, W. J. D. *Microstruct. Sci.* **1994**, *21*, 95.
- (14) Shaw, W. J. D.; Pan, J.; Growler, M. A. In *Proceedings of the 2nd International Conference on Structural Applied Mechanics in Alloying*; DeBarbadillo, J. J., Fores, F. H., Schwarz, R., Eds.; ASM International: Materials Park, OH, 1993; p 431.
- (15) Castricum, H. L.; Yang, H.; Bakker, H.; Deursen, J. H. V. *Mater. Sci. Forum* **1997**, *235–238*, 211.
- (16) Farrell, M. P.; Kander, R. G.; Aning, A. O. *J. Mater. Synth. Proc.* **1996**, *4*, 1996.
- (17) Font, J.; Muntasell, J.; Cesari, E. *Mater. Res. Bull.* **1999**, *34*, 157.
- (18) Ishida, T. *J. Mater. Sci. Lett.* **1994**, *13*, 623.
- (19) Balik, C. M.; Bai, C.; Koch, C. C.; Spontak, R. J.; Saw, C. K. *Mater. Res. Soc. Symp. Proc.* **1997**, *461*, 39.
- (20) Bai, C.; Spontak, R. J.; Koch, C. C.; Saw, C. K.; Balik, C. M. *Polymer*, in press.
- (21) Smith, A. P.; Spontak, R. J.; Ade, H.; Smith, S. D.; Koch, C. C. *Adv. Mater.* **1999**, *11*, 1277.
- (22) Smith, A. P.; Spontak, R. J.; Balik, C. M.; Koch, C. C.; Smith, S. D.; Ade, H. *Macromolecules*, submitted.
- (23) Smith, A. P.; Shay, J. S.; Spontak, R. J.; Balik, C. M.; Ade, H.; Smith, S. D.; Koch, C. C. *Polymer*, in press.

- (24) Smith, A. P.; Spontak, R. J.; Koch, C. C.; Ade, H. *Macromol. Mater. Eng.* **2000**, 274, 1.
- (25) Ade, H. In *Vacuum Ultraviolet Spectroscopy II*; Samson, J., Ederer, D., Eds.; Academic Press: San Diego, 1998; Vol. 32, pp 225–262.
- (26) Feser, M.; Carlucci-Dayton, M.; Jacobsen, C.; Kirz, J.; Neuhäusler, U.; Smith, G.; Yu, B. *SPIE Proc.* **1998**, 3449, 19.
- (27) Du, Y.; Xue, Y.; Frisch, H. L. In *Physical Properties of Polymers Handbook*; Mark, J. E., Ed.; American Institute of Physics: Woodbury, NY, 1996; p 227.
- (28) All STXM images in which PI appears dark are compared with their complement in which PMMA appears dark to avoid erroneous interpretation.
- (29) Bucknall, C. B. *Toughened Plastics*; Applied Science Publishers: London, 1977.
- (30) Partridge, I. K. In *Multicomponent Polymer Systems*; Miles, I. S., Rostami, S., Eds.; Longman Scientific and Technical: Essex, England, 1992; p 149.
- (31) Walker, I.; Collyer, A. A. In *Rubber Toughened Engineering Plastics*; Collyer, A. A., Ed.; Chapman & Hall: London, 1994; p 29.
- (32) Bucknall, C. B. In *The Physics of Glassy Polymers*, 2nd ed.; Haward, R. N., Young, R. J., Eds.; Chapman and Hall: New York, 1997.

MA9915475